THE JOURNAL OF PHYSICAL CHEMISTRY A

ARTICLE

pubs.acs.org/JPCA

# NMR Study of Conformational Exchange and Double-Well Proton Potential in Intramolecular Hydrogen Bonds in Monoanions of Succinic Acid and Derivatives

Jing Guo,[†] Peter M. Tolstoy,[*,†,‡,§] B. Koeppe,[†] Gleb S. Denisov,[‡] and Hans-Heinrich Limbach[†]

[†]Institute of Chemistry and Biochemistry, Free University of Berlin, Takustrasse 3, D-14195 Berlin, Germany

[‡]V. A. Fock Institute of Physics and [§]Department of Chemistry, St. Petersburg State University, St. Petersburg 198504, Russia

Supporting Information

**ABSTRACT:** We present a $^{1}H$, $^{2}H$, and $^{13}C$ NMR study of the monoanions of succinic (**1**), *meso*- and *rac*-dimethylsuccinic (**2**, **3**), and methylsuccinic (**4**) acids (with tetraalkylammonium as the counterion) dissolved in $CDF_3/CDF_2Cl$ at 300−120 K. In all four monoanions, the carboxylic groups are linked by a short intramolecular OHO hydrogen bond revealed by the bridging-proton chemical shift of about 20 ppm. We show that the flexibility of the carbon skeleton allows for two gauche isomers in monoanions **1**, **2**, and **4**, interconverting through experimental energy barriers of 10−15 kcal/mol (the process itself and the energy barrier are also reproduced in MP2/6-311++G** calculations). In **3**, one of the gauche forms is absent because of the steric repulsion of the methyl groups. In all four monoanions, the bridging proton is located in a double-well potential and subject, at least to some extent, to proton tautomerism, for which we estimate the two proton positions to be separated by ca. 0.2 Å. In **1** and **3**, the proton potential is symmetric. In **2**, slowing the conformational interconversion introduces an asymmetry to the proton potential, an effect that might be strong enough even to synchronize the proton tautomerism with the interconversion of the two gauche forms. In **4**, the asymmetry of the proton potential is due to the asymmetric substitution. The intramolecular H-bond is likely to remain intact during the interconversion of the gauche forms in **1**, **3**, and **4**, whereas the situation in **2** is less clear.

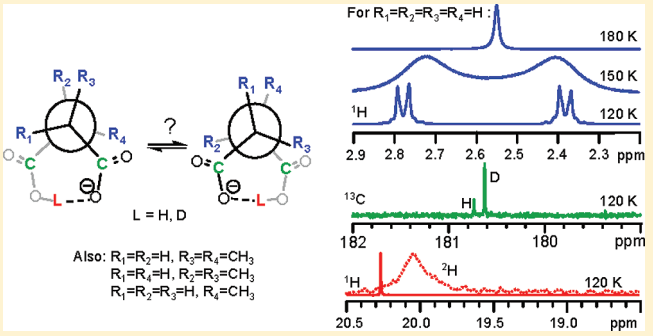


## INTRODUCTION

The geometry, flexibility, and energetics of short strong hydrogen bonds have been the subjects of many studies in recent decades. Special interest is drawn toward intramolecular complexes, because they seemingly provide better control over the relative orientation of the donor and acceptor groups. Moreover, in many such systems, the equilibrium is almost entirely shifted toward hydrogen-bond formation, a condition that is rarely fulfilled among intermolecular complexes. Monoanions of dicarboxylic acids are considered to be good candidates for forming short intramolecular hydrogen bonds because of the closely matched $pK_a$ values of the carboxylic groups and their steric proximity.[1,2] The most extensively studied among them are perhaps the symmetric species hydrogen maleate and hydrogen phthalate, in which the rigid C=C bonds ensure an orientation of the carboxylic groups favorable for the formation of intramolecular hydrogen bonds. X-ray diffraction measurements show that the O···O distance is 2.40−2.42 Å for hydrogen maleate[3,4] and 2.40−2.55 Å for hydrogen phthalate,[5,6] depending on the counterion. The shape of the proton potential and the equilibrium proton position in such a short hydrogen bridge are affected by the symmetry of the environment. For example, neutron scattering experiments revealed a central proton position in the case of a symmetric placement of the counterion ($K^+$) in hydrogen maleate[7] and an asymmetric proton position in the case of an asymmetric location of $K^+$ for hydrogen phthalate.[5] In aprotic solvents such as dimethyl sulfoxide (DMSO), tetrahydrofuran (THF), $CD_3CN$, and $CD_2Cl_2$, the intramolecular hydrogen bond is usually retained, as indicated by the low-field $^{1}H$ NMR chemical shift of the bridging proton.[1,8−10] However, the symmetry of the hydrogen bond in liquid solutions is more ambiguous, first, because experimental evidence is usually of indirect spectroscopic nature and, second, because the mobility of the surrounding solvent molecules creates an instantaneous asymmetry of the environment that makes the equilibrium position of the proton time-dependent. For example, the bridging-proton chemical shift of hydrogen malonate dissolved in DMSO covers an unusually broad range of 9−20 ppm, depending on the countercation, indicating a strong influence of the latter on the H-bond geometry and symmetry.[10] Another example is hydrogen maleate dissolved in aprotic solvents, where the primary H/D isotope effects on chemical shifts are evidence for a single

**Received:** February 1, 2011
**Revised:** August 1, 2011
**Published:** August 02, 2011

central proton position,[11] whereas secondary $^{16}O/^{18}O$ isotope effects on carboxylic carbon chemical shifts seem to indicate a tautomeric proton exchange between two asymmetric structures.[1,2] The proton position in the hydrogen bridge correlates strongly with the heavy-atom distance: neutron diffraction studies have shown that the central proton positions coincide with shortest heavy-atom distances.[12] This suggests that proton tautomerism in intramolecular hydrogen bonds might be related to the heavy-atom distances being constrained by the molecular skeleton.

Summarizing all of the above evidence, in the monoanions of dicarboxylic acids, the formation, stability, geometry, and dynamics of hydrogen bonds respond sensitively to the changes in the molecular core and surroundings. In this work, we explore the implications of the flexibility of the molecular skeleton. For this purpose, we have chosen the monoanions of succinic acid and its derivatives. The molecular skeletons of these acids are constructed by single carbon−carbon bonds, and thus, the resulting nonplanar structures of the monoanions are not only more flexible in comparison with those of maleic and phthalic acid, but also could exist in three canonical rotamers, as shown in Figure 1. The questions arise: Which structures are the most stable in polar aprotic environments? Which hydrogen-bond geometry do these molecules adopt? Which hydrogen-bond dynamics will possibly be retained?

In the solid state, monoanions of succinic acid and its derivatives usually form infinite chains; that is, their hydrogen bonds are intermolecular, linking carboxylic groups of two neighboring molecules (in either trans or gauche form).[13−15] As a combination of experiments and theoretical calculations shows, in a non-hydrogen-bonding medium such as the gas phase,[16] liquid aprotic solutions,[16,17] or liquid crystals,[18] isolated monoanions of succinic acid exist predominantly in gauche form with an intramolecular OHO hydrogen bond. Such an intramolecular H-bond was even postulated for methylsuccinic acid in aqueous solution at pH < 4.[19]

One of the most informative methods for studying the structures of monoanions of succinic acid and its derivatives in liquid solutions is NMR spectroscopy. Previously, the values of $^{1}H$ and $^{13}C$ chemical shifts, H/D isotope effects thereupon, and $^{3}J(HH)$ scalar couplings were used to determine the conformation.[20−22]

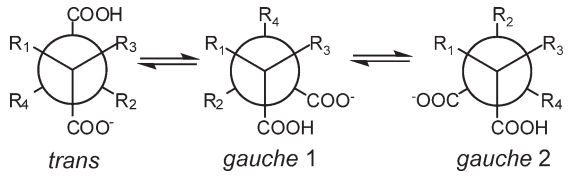


**Figure 1.** Possible conformers of a monoanion of succinic acid or its derivatives.

However, little is known about the proton position in the intramolecular H-bonds and the possible interconversion between the gauche 1 and gauche 2 conformers, which are degenerate in many cases. Such an exchange could occur either directly, retaining the H-bond, or through the trans conformation, which would require breaking of the H-bond.

The main goal of this work was to address three questions: (1) Is a truly symmetric H-bond formed if more flexibility is allowed in the skeleton of the dicarboxylic acid monoanion? (2) Is the interconversion of the gauche forms possible for monoanions of succinic acid and its derivatives? (3) Does the interconversion require breaking of the intramolecular H-bond?

To answer these questions, we used low-temperature NMR spectroscopy to study tetraethylammonium (TEA) hydrogen succinate (**1**), tetramethylammonium (TMA) hydrogen *meso*-dimethylsuccinate (**2**), TMA hydrogen *rac*-dimethylsuccinate (**3**), and TEA hydrogen *R*-(+)-methylsuccinate (**4**) dissolved in liquefied freonic mixture ($CDF_3/CDF_2Cl$) as a polar aprotic solvent. Structures of the studied complexes with intramolecular H-bonds are shown schematically in Figure 2. The systems selected for this study can be considered as representing the somewhat general case of two carboxylates in close proximity in an aprotic environment, such as two side chains of glutamic and/or aspartic acids in the interior of a protein.[23]

Matched (as in **1**−**3**) or close (as in **4**) proton-donating abilities of the pairs of carboxylate residues and bulky noninteracting tetraalkylammonium counterions provide most favorable conditions for the formation of strong hydrogen bonds. As mentioned above, we expect certain structural flexibility in **1**−**4**, namely, rotation about the central C−C bond, that could lead to a conformational interconversion between the two gauche forms. Also, steric factors, especially repulsion of the methyl substituents, might influence the conformational preferences. A similar effect was shown previously for α,α′-di-*tert*-butylsuccinic acid, where the meso isomer is exclusively in the trans form whereas the racemic isomer can adopt the gauche conformation and its monoanion does form an intramolecular H-bond in an aprotic medium.[24]

For **1**−**4**, we have determined the $^{1}H$ and $^{13}C$ chemical shifts, as well as the H/D isotope effects on them.[11,25,26] NMR signals in the temperature range of 300−120 K were subjected to line shape analysis. Previously established NMR correlations were used to estimate hydrogen-bond geometries.[12,25,27] Additionally, we performed some theoretical calculations to support our interpretation of the experimental NMR spectra.

## EXPERIMENTAL PROCEDURES

Succinic acid, *meso*-/*rac*-2,3-dimethylsuccinic acid, *meso*-2,3-dimethylsuccinic acid, and (*R*)-(+)-methylsuccinic acid were

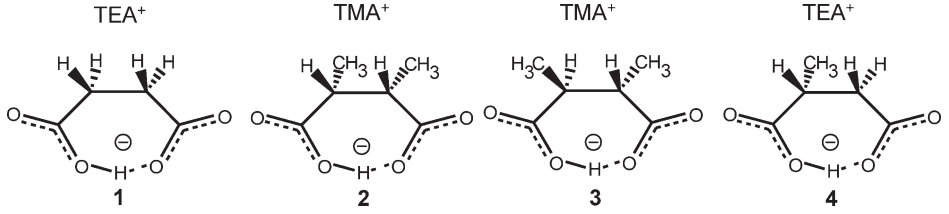


**Figure 2.** Structures of the dicarboxylic acid monoanions studied in this work: tetraethylammonium (TEA) hydrogen succinate (**1**), tetramethylammonium (TMA) hydrogen *meso*-dimethylsuccinate (**2**), hydrogen *rac*-dimethylsuccinate (**3**), and tetraethylammonium hydrogen *R*-(+)-methylsuccinate (**4**).


dx.doi.org/10.1021/jp201073j |*J. Phys. Chem. A* 2011, 115, 9828–9836

purchased from Aldrich. Their corresponding salts were prepared by mixing a $CH_2Cl_2$ solution of the above acids with 1 equiv of tetraethylammonium or tetramethylammonium hydroxide solution (~1.5 M in $CH_3OH$, Fluka). $H_2O$ and $CH_3OH$ were removed by repeated additions of dry $CH_2Cl_2$ (2−3 mL) to the reaction mixture, followed each time by evaporation under reduced pressure using a rotary evaporator. All studied monoanions were deuterated in the mobile proton sites by dissolving them twice in $CH_3OD$ and removing the solvent under reduced pressure. Then, the necessary amounts were weighed in thick-walled NMR sample tubes equipped with J. Young polytetrafluoroethylene (PTFE) valves (Wilmad). A final deuteration step was performed by adding $CH_3OD$ directly into the sample tube and removing the solvent under high vacuum for ca. 12 h. At the end, a $CDF_3/CDF_2Cl$ mixture was added as the solvent by vacuum transfer. The $CDF_3/CDF_2Cl$ mixture was synthesized according to a modification of the procedure of Siegel and Anet.[28] The solute concentration was about 0.02 M in all samples.

Ab initio calculations were carried out using the Gaussian 03 package.[29] Full geometry optimizations and harmonic frequency calculations of compounds **1**−**4** (without countercations) in a vacuum were performed using the MP2 method with the 6-311++G** basis set. Transition states were found using the QST2 and QST3 algorithms built into the Gaussian package.

Line shape simulations were performed using either the free Mexico 3 code[30] written by A. D. Bain or by the gNMR software[31] developed by P. H. M. Budzelaar.

Chemical shifts were measured using $CHF_2Cl$ and $CDF_2Cl$ as internal standards and converted to the conventional TMS scale: $\delta(C\underline{H}F_2Cl) = 7.18$ ppm, $\delta(\underline{C}DF_2Cl) = 117.37$ ppm.

## RESULTS

$^1H$ (solid line), $^2H$ (dotted line), and $\{^1H\}^{13}C$ NMR spectra of the samples containing 0.02 M solutions of partially deuterated **1**−**4** dissolved in $CDF_3/CDF_2Cl$ measured at low temperatures down to 120 K are shown in Figures 3−5. The dashed lines are results of spectral simulations and will be discussed later. In the following subsections, we present the data for each species individually.

**TEA Hydrogen Succinate (1).** In Figure 3, the low-field parts of the $^1H$ and some $^2H$ NMR spectra (Figure 3a); the high-field parts of the $^1H$ NMR spectra, containing the signals of the aliphatic protons (Figure 3b); and the carbonyl regions of the corresponding $\{^1H\}^{13}C$ NMR spectra (Figure 3c) of the sample containing **1** are shown.

**TMA Hydrogen Dimethylsuccinate (Meso Form 2 and Racemic Form 3).** In Figure 4, the NMR spectra of the sample containing a mixture of **2** and **3** are shown in a similar manner as was done for **1** in Figure 3. The high-field regions of the $^1H$ NMR spectra (Figure 4b) are split into two parts, containing the signals of methine CH and methyl $CH_3$ protons, respectively. The assignment of the signals to monoanions **2** and **3** was made by comparison with results obtained from an additional sample containing only the monoanion of *meso*-2,3-dimethylsuccinic acid (**2**; results not shown). Pure racemic form **3** was not commercially available.

**TEA Hydrogen Methylsuccinate (4).** In Figure 5, parts of the $^1H$, $^2H$, and $\{^1H\}^{13}C$ NMR spectra of the sample containing **4** are shown. The quality of the $^2H$ NMR spectrum is very poor, and the deuteron chemical shifts cannot be safely established.

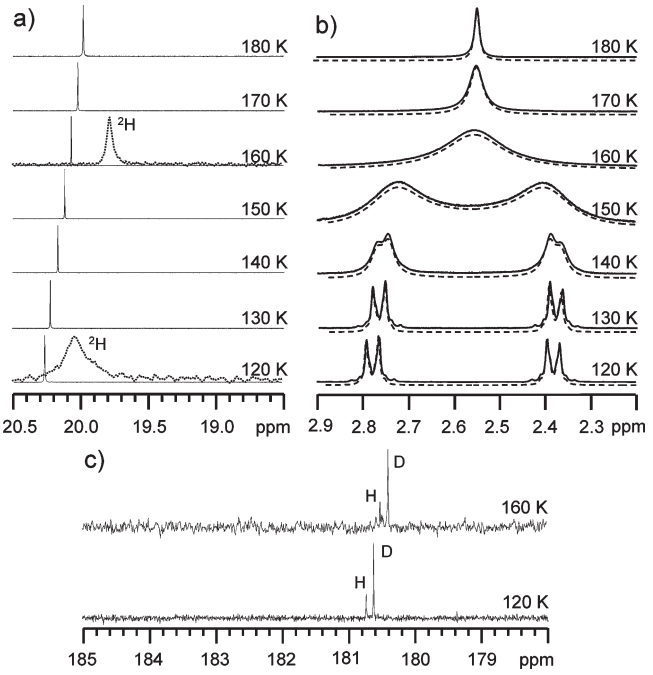


**Figure 3.** NMR spectra of a sample containing a 0.02 M solution of **1** in $CDF_3/CDF_2Cl$. (a) Low-field parts of $^1H$ (solid lines) and $^2H$ (dotted lines) spectra; (b) high-field parts of $^1H$ spectra (solid lines), together with line shape analysis (dashed line; see Discussion for more details); (c) low-field parts of $\{^1H\}^{13}C$ NMR spectra. $^{13}C$ signals from the protonated and deuterated forms are marked H and D, respectively.

However, the sign of the primary H/D isotope effect on the chemical shift is clearly negative, $\delta D - \delta H < 0$. The asterisks [single (*) and double (**)] are used to arbitrarily distinguish two forms of the monoanion whose specific structures will be addressed in the Discussion section.

NMR parameters for all monoanions obtained from the spectra shown in Figures 3−5 are collected in Table 1. The following notation is used: $\delta H$ and $\delta D$ are the chemical shifts of the bridging proton and deuteron, respectively. $\delta(\underline{C}OHOC)$ and $\delta(COHO\underline{C})$ are the chemical shifts of the two carboxylic carbon nuclei; when a proton is substituted for a deuteron, the corresponding carboxylic carbon chemical shifts are denoted as $\delta(\underline{C}ODOC)$ and $\delta(CODO\underline{C})$. Because of symmetry, only in the cases of **2** and **4** are the chemical shifts $\delta(\underline{C}OHOC)$ and $\delta(COHO\underline{C})$ different. For **1** and **3** we observe only one carboxylic carbon signal, assigned to both $\delta(\underline{C}OHOC)$ and $\delta(COHO\underline{C})$.

**Line Shape Analysis.** As can be seen from Figures 3b, 4b, and 5b, the line shapes of the signals of the aliphatic protons in **1**, **2**, and **4** are subject to strong temperature dependencies, whereas the line shape of the corresponding signal of **3** is almost invariant with temperature, and only the chemical shifts are somewhat temperature-dependent. As we demonstrate in the following paragraphs, for **1**, **2**, and **4**, the line shape changes can be simulated assuming a two-state chemical exchange. The underlying physical process is addressed in the Discussion section. In this section, we present only the results of the simulation. In all cases, we have estimated the natural linewidths of the exchanging lines and their splitting patterns from the spectra measured at the lowest temperatures. In addition, we have assumed that the intrinsic chemical shifts depend linearly on temperature.

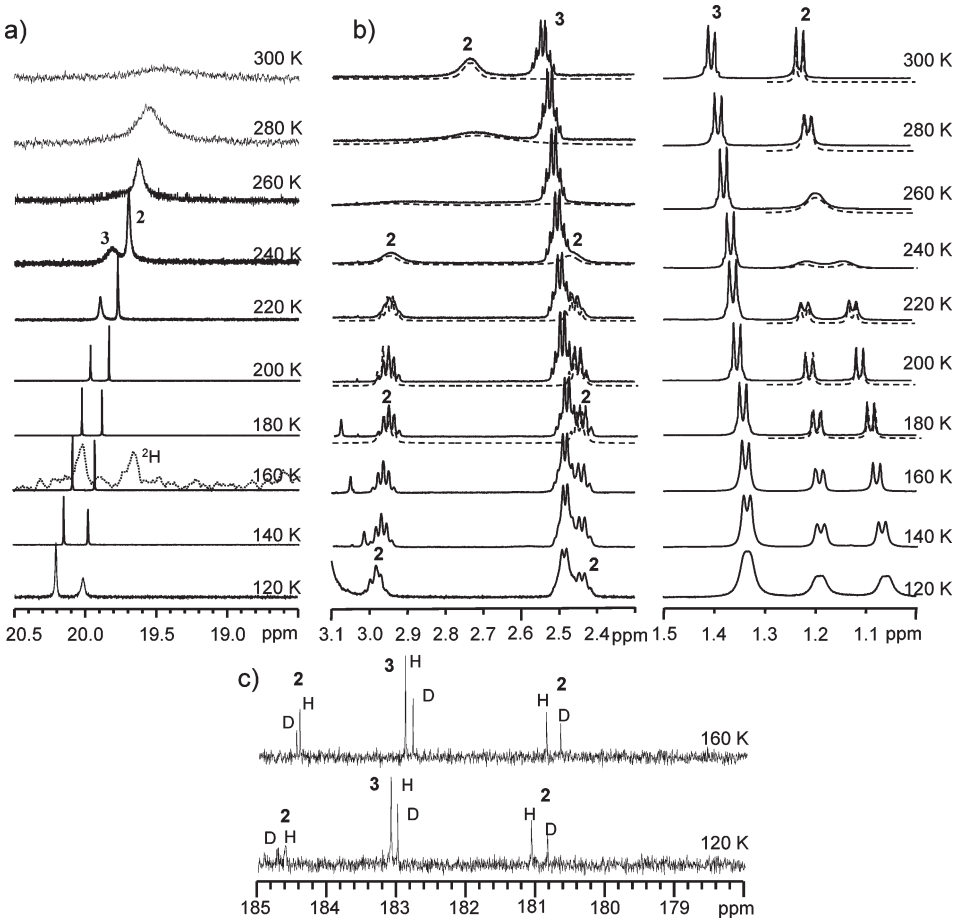


**Figure 4.** NMR spectra of a sample containing a 0.02 M solution of a mixture of **2** and **3** in $CDF_3/CDF_2Cl$. (a) Low-field parts of $^1$H (solid lines) and $^2$H (dotted lines) spectra; (b) high-field parts of $^1$H NMR spectra, containing signals of methine CH (left) and methyl $CH_3$ (right) protons, with the results of the line shape analysis indicated by dashed lines (see Discussion for more details); (c) low-field parts of $\{^1H\}^{13}C$ NMR spectra. $^{13}$C signals from the protonated and deuterated forms are marked H and D, respectively.

In the spectra of **1**, the sharp singlet at 2.54 ppm visible at 180 K broadens upon cooling; splits into two signals below 160 K; and finally, at 120 K, transforms into a pair of doublets split by 13.9 Hz. The result of the line shape analysis assuming a symmetric two-state AA′BB′ ⇌ BB′AA′ exchange is shown in Figure 3b as dashed lines.

The methine proton signals of **2** (Figure 4b, left) are transformed from a broad singlet at 300 K into a pair of multiplets at 160 K with coalescence at ca. 270 K. The methyl proton signals (Figure 4b, right) are transformed upon cooling from a doublet into a pair of doublets split by 7.5 and 7.2 Hz, with coalescence at ca. 250 K. We analyzed these temperature dependencies assuming also, as in **1**, a symmetric two-state $ABX_3Y_3 \rightleftharpoons BAY_3X_3$ chemical exchange for methine (A, B) and methyl ($X_3$, $Y_3$) protons. We simulated these two regions separately, and the results of the fits are shown as dashed lines in Figure 4b.

The line shapes of the methine and methyl proton signals of **3** do not change upon cooling. Apparently, the chemical exchange that is possible for **2** is hindered for **3**.

Upon lowering the temperature, the methyl proton signals of **4** (Figure 5b, right) are transformed from a doublet into a pair of doublets of unequal intensity (2:3) split by 6.4 and 7.2 Hz. Coalescence occurs at ca. 190 K. Fitting was done only for the methyl proton signals, assuming an asymmetric two-state ($X_3$, $Y_3$) exchange according to an $ABCX_3 \rightleftharpoons DEFY_3$ exchange scheme. For simplicity, we report here only the larger of the two rate constants resulting from these simulations, calling it $k_{CH_3}$ and not making a distinction between "forward" and "backward" reaction rates in the text. The other rate constant can be found by multiplying $k_{CH_3}$ by the signal intensity ratio, that is, 0.66. As shall become clear in the Discussion section, this information serves our goals sufficiently well.

All rate constants obtained from the line shape analyses are listed in Table 2.

In Figure 6, an Arrhenius plot of the rate constants from Table 2 is shown. The activation energies and pre-exponential factors of the exchange processes, obtained by linear fitting of the data points, are collected in Table 3. We note that, for **2**, the activation energies obtained by two independent fits coincide within the margin of error.

## DISCUSSION

The low-field chemical shifts of the OH protons in **1**−**4** (ca. 20 ppm, see Figures 3−5) indicate the formation of short hydrogen bonds.[1] The proton signals are concentration-independent, and no new signals appear after the partial deuteration of the sample.[32] These findings support the conclusion that these

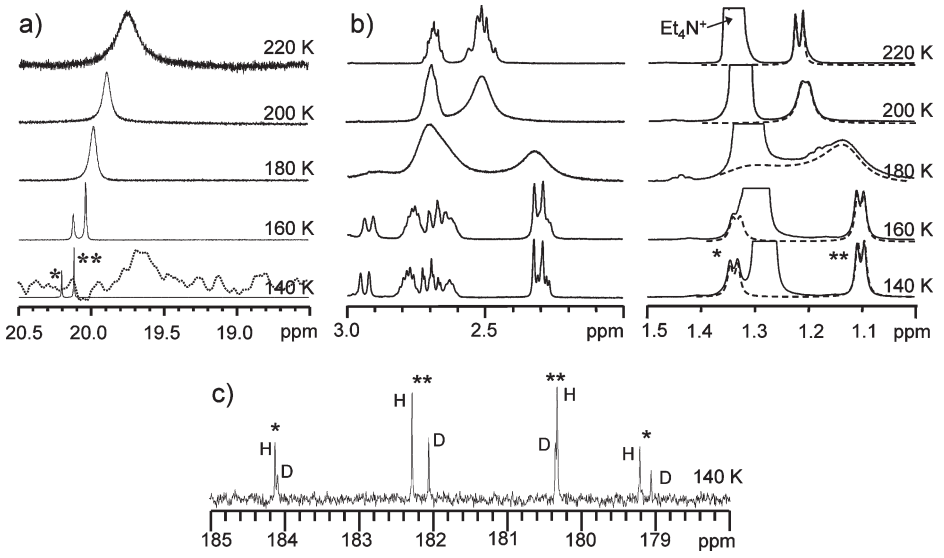


**Figure 5.** NMR spectra of a sample containing a 0.02 M solution of **4** in $CDF_3/CDF_2Cl$. (a) Low-field parts of $^1H$ (solid lines) and $^2H$ (dotted lines) spectra; (b) high-field parts of $^1H$ NMR spectra, containing signals of CH (left) and $CH_3$ (right) protons, with the results of the line shape analysis indicated by dashed lines (see Discussion for more details); (c) $\{^1H\}^{13}C$ NMR spectra. $^{13}C$ signals from the protonated and deuterated forms are marked H and D, respectively. The asterisks [single (*) and double (**)] are used to arbitrarily distinguish the gauche 1 and gauche 2 forms of the monoanion (this interpretation is confirmed in the Discussion).

**Table 1. $^1H$, $^2H$, and $^{13}C$ NMR Chemical Shifts and H/D Isotope Effects for 1−4, Obtained from Spectra Shown in Figures 3−5 for Selected Temperatures**

| compound | $T$ (K) | $\delta$H (ppm) | $\delta$D (ppm) | $\delta$D − $\delta$H (ppm) | $\delta$(COHOC) (ppm) | $\delta$(COHOC) (ppm) | $\delta$(CODOC) − $\delta$(COHOC) (ppm) | $\delta$(CODOC) − $\delta$(COHOC) (ppm) |
|---|---|---|---|---|---|---|---|---|
| **1** | 120 | 20.27 | 20.06 | −0.21 | 180.74 | 180.74 | −0.11 | −0.11 |
| | 160 | 20.07 | 19.78 | −0.29 | 180.51 | 180.51 | −0.12 | −0.12 |
| **2** | 120 | 20.02 | | | 181.08 | 184.61 | −0.23 | 0.11 |
| | 160 | 19.93 | 19.65 | −0.28 | 180.88 | 184.42 | −0.20 | 0.04 |
| **3** | 120 | 20.21 | | | 183.09 | 183.09 | −0.09 | −0.09 |
| | 160 | 20.08 | 20.01 | −0.07 | 182.91 | 182.91 | −0.11 | −0.11 |
| **4**(*) | 140 | 20.21 | ∼19.6 | ∼−0.6 | 184.12 | 182.28 | −0.03 | −0.22 |
| **4**(**) | 140 | 20.12 | ∼19.6 | ∼−0.5 | 179.22 | 180.33 | −0.15 | 0.02 |

**Table 2. Rate Constants of the Exchange Processes in 1, 2, and 4 at Various Temperatures, As Determined by the Line Shape Analyses Shown in Figures 3−5 (Dashed Lines)**

| **1** | | **2** | | | **4**[a] | |
|---|---|---|---|---|---|---|
| $T$ (K) | $k$ (Hz) | $T$ (K) | $k_{CH}$ (Hz) | $k_{CH_3}$ (Hz) | $T$ (K) | $k_{CH_3}$ (Hz) |
| 120 | 0.09 | 180 | 0.002 | 0.003 | 140 | 2.38 |
| 130 | 1.7 | 200 | 0.02 | 0.03 | 160 | 68.2 |
| 140 | 35 | 220 | 0.8 | 1.3 | 180 | 930 |
| 150 | 205 | 240 | 26 | 37 | 200 | 12300 |
| 160 | 830 | 260 | 200 | 193 | 220 | 73700 |
| 170 | 3600 | 280 | 1490 | 1040 | | |
| 180 | 17000 | 300 | 17300 | 12200 | | |

[a] In **4**, the exchange is asymmetric, and $k_{CH_3}$ represents the larger of the forward and backward reaction rates.

H-bonds are intramolecular and justify the structures of the studied monoanions as shown in Figure 2. Geometric and energetic properties of the intramolecular hydrogen bonds are the focus of our study. This section is structured as follows: First, we discuss the physical process leading to the two-state chemical exchange in the NMR spectra of **1**, **2**, and **4**, in contrast to the absence of such in **3**. Second, we estimate the geometry of the intramolecular hydrogen bond in all studied monoanions and support these estimations by some quantum mechanical calculations. Finally, we address the question of whether the intramolecular hydrogen bond is retained during conformational exchange.

**Conformational Exchange in Monoanions of Succinic, Methylsuccinic, and Dimethylsuccinic Acids.** As pointed out in the Introduction, the monoanions of succinic acids can exist as three rotamers.[22] It was also mentioned that the trans conformer is virtually absent in polar aprotic solvents, even at room temperature, because of the stabilization of the gauche conformers by the strong intramolecular hydrogen bonds. Thus, it is reasonable to assume that the temperature dependence of the $^1H$ NMR chemical shifts of the aliphatic protons of **1**, **2**, and **4** arises from the interconversion of the gauche 1 and gauche 2 forms, which


dx.doi.org/10.1021/jp201073j |J. Phys. Chem. A 2011, 115, 9828–9836

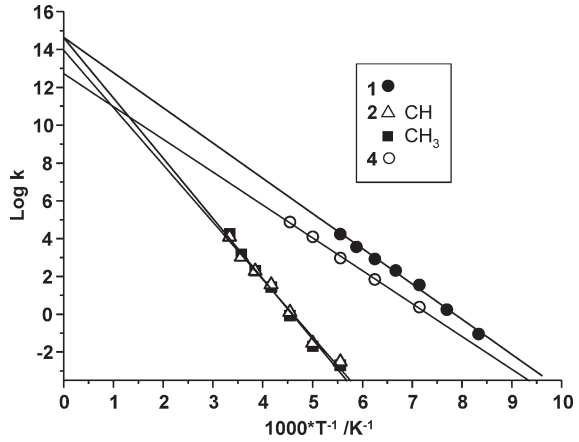


**Figure 6.** Arrhenius diagram for the two-state chemical exchange process in **1**, **2**, and **4**; data points were obtained from Table 2. The parameters of the linear fitting are given in Table 3.

**Table 3. Activation Energies and Pre-exponential Factors of the Chemical Exchange Processes in 1, 2, and 4, Obtained by Linear Fitting of the Data Points Shown in Figure 6**

| | signals used for the line shape analysis | $E_a$ (kcal·mol$^{-1}$) | $A$ (s$^{-1}$) |
|---|---|---|---|
| **1** | methylene protons | 8.5 ± 0.2 | $4.3 \times 10^{14}$ |
| **2** | methine protons | 13.8 ± 0.6 | $9.0 \times 10^{13}$ |
| | methyl protons | 14.6 ± 0.7 | $4.2 \times 10^{14}$ |
| **4** | methyl protons | 8.0 ± 0.2[a] | $5.3 \times 10^{12}$ [a] |

[a] Values obtained by fitting the data for the larger value of two rate constants for an asymmetric exchange process.

differ mostly in terms of the sign of the dihedral C−C−C−C angle. In this section, we refer to this rocking motion as "conformational interconversion" along the single C−C bond. This process is schematically shown in Figure 7. We consider the details of the exchange for each of the monoanions separately.

The fast conformational interconversion in **1** converts the AA′BB′ spin system of the CH protons into an effective $A_4$ spin system. The two carboxylic carbons of **1** stay chemically equivalent at all exchange rates. This observation confirms that the bridging proton of the intramolecular OHO bond does not reside close to one of the carboxylic groups, but is either exactly in the hydrogen-bond center, as in O···H···O, or jumps rapidly between two positions, as in O−H···O ⇄ O···H−O. Both situations would render the two carbon atoms equivalent. Indeed, if the proton were staying closer to only one of the carboxylic groups, as in O−H···O, the effective symmetry of the monoanion could not be higher than $C_s$ (meaning an $A_2B_2$ spin system of the CH protons), whereas experimentally, the effective symmetry is $C_{2v}$ at higher temperatures. In the next subsection, we further address the question of the equilibrium proton position (true symmetry versus rapid jumps) considering primary and secondary H/D isotope effects.

Carboxylic carbons of **2** give rise to two signals at the lowest temperatures. With increasing temperature, the spin system of the CH and $CH_3$ protons is converted from $ABX_3Y_3$ into $AA'X_3X'_3$. These findings, unfortunately, do not allow for a distinction between the cases of the proton in the hydrogen-bond center, in a double-well potential, or even in an asymmetric single well (close to one of the carboxylic groups, but jumping

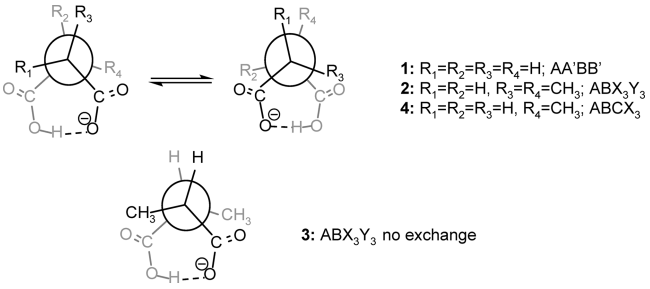


**Figure 7.** Schematic representation of the conformational exchange process of **1**−**4** and the spin labels used in the line shape analyses. Atoms (groups) in black are closer to the reader, whereas those in gray are farther away when viewed along the C−C single bond. Here, proton positions in the intramolecular OHO hydrogen bonds were chosen arbitrarily.

concertedly with the conformational interconversion). We leave this question until the next subsection.

In **3**, the line shapes of the methine (Figure 4b, left) and methyl (Figure 4b, right) proton signals do not change with temperature. This indicates the existence of only one stable gauche form of **3** with an effectively symmetric intramolecular hydrogen bond (central-symmetric single well or symmetric double well). What causes the other gauche form to be so unstable? We believe that the direct cause is the steric repulsion of methyl groups. Indeed, the two gauche forms are neither perfectly staggered nor perfectly eclipsed because of the intramolecular hydrogen bond. Ab initio calculations (see the Supporting Information) and the $^3J$(HH) scalar coupling of about 7 Hz strongly suggest that the C−C−C−C dihedral angle is significantly larger than 60°. This means that, in one of the gauche forms, the methyl groups are well separated, facing in different directions (as shown in the Figure 7), whereas in the other gauche conformation, they would point in almost the same direction and thus would sterically repulse (not shown). In other words, the energy gain provided by the intramolecular H-bond would be (over)compensated by the destabilization due to the steric repulsion of the methyl substituents.

Monoanion **4** is the least symmetric among the studied species. Neither fast conformational interconversion nor a possible fast bridging-proton migration in the H-bond could significantly change the symmetry of the molecule. Moreover, in **4**, the exchange between the gauche 1 and gauche 2 forms is nondegenerate (equilibrium constant not equal to 1). Thus, we observe two sets of signals of **4** at low temperatures (marked with single and double asterisks, Figure 5a,b) with a ratio of integrated intensities equal to 2:3. The two carboxylic carbon atoms are chemically nonequivalent in each of the gauche forms regardless to the position of the bridging proton and thus all together four carbon signals are visible at 140 K.

**Hydrogen-Bond Symmetry in 1−4.** The first question to address is whether the bridging proton in the studied monoanion is located in the geometric center of the H-bond. One of the parameters often considered in this context is the sign of the primary H/D isotope effect on the chemical shift, defined as $\delta D - \delta H$.[11] A positive value of this quantity means that the deuteron is less shielded than the proton, which is usually the case in symmetric single-well potentials because of the smaller amplitude of the asymmetric proton stretching vibration.[33] Although the meaning of a positive value is sometimes ambiguous,[2,11]

it remains well accepted that a negative value indicates a double-well or asymmetric single-well potential. In all cases studied in this work, the sign of the primary H/D isotope effect on the chemical shift is clearly negative, and thus, the possibility of a central-symmetric proton position can be safely ruled out. Furthermore, the presence of only one signal for the two carboxylic groups in each **1** and **3** supports the conclusion that, in both species, the proton jumps rapidly between two equivalent positions, rendering the carboxylic carbon atoms chemically equivalent. In **2** and **4**, the situation is less clear because these monoanions have lower symmetry than **1** and **3**, and thus, the carboxylic carbon atoms would remain nonequivalent even if the proton migrated rapidly between two positions.

Nevertheless, some additional information concerning proton motion can be extracted from the $^{13}$C NMR spectra. It was demonstrated in ref 25 that the H/D isotope effects on carboxylic carbon chemical shifts change sign when the proton crosses the H-bond center: it is negative and has large absolute values for COO−H···O$^-$ complexes, whereas it is positive and has smaller absolute values for COO$^-$···H−O complexes. In the case of proton tautomerism in a symmetric double-well potential, COO−H···O$^-$ ⇄ COO$^-$···H−O, the average H/D isotope effect is negative.[25]

In **2**, when the isomerization is slowed at low temperatures, the H/D isotope effects on the carboxylic carbon chemical shifts have opposite signs (−0.20 and +0.04 ppm at 160 K), which indicates that the proton predominantly resides on one side of the H-bond. The nonequivalence of the carboxylic groups is apparently sufficient to induce such a preference. Even if proton tautomerism occurred, the equilibrium constant would still be significantly different from unity. This means that, when **2** undergoes conformational interconversion between the gauche 1 and gauche 2 forms—and thus the carboxylic carbon atoms exchange their chemical environments—the bridging proton is likely to jump. Interestingly, the absolute values of the carboxylic carbon chemical shifts are almost 4 ppm apart, which is comparable to the full protonation/deprotonation shift of the carboxylic carbon signal.[34]

In **4**, even though the chemical difference between the two carboxylic groups is significant, the preference of the bridging proton to reside on one or on the other side of the hydrogen bond depends on the conformation of the monoanion. In the ** form, the H/D isotope effects on the carboxylic carbon chemical shifts have opposite signs, suggesting a strong preference of the proton for one of the carboxylic groups, similar to what was observed for **2**. In the * form of **4**, both isotope effects are negative, indicating that the bridging proton is likely to jump more evenly back and forth between two sites.

In this subsection, we addressed only distinct proton tautomers for **1**−**4**. However, it is reasonable to assume that, in reality, in solution, there is a distribution of "solvatomers"[9] that differ by the structures of their solvation shells and thus bear different equilibrium proton positions. Moreover, each of the gauche forms is probably present also as an ensemble of solvatomers, distinguished by minute changes of the C−C−C−C dihedral angle. Nevertheless, for the sake of simplicity, we consider only two gauche forms and two proton tautomers, as the most representative members of their corresponding ensembles.

**Hydrogen-Bond Geometry in 1−4.** Now, we attempt to quantitatively estimate H-bond geometries using previously published hydrogen-bond correlations that take into account the qualitative symmetry considerations discussed in the preceding subsection. It was shown by neutron scattering measurements that for an OHO complex the $r_{OH}$ and $r_{HO}$ distances or their linear combinations

$$q_1 = \frac{1}{2}(r_{OH} - r_{HO}) \quad \text{and} \quad q_2 = r_{OH} + r_{HO} \tag{1}$$

are related.[12] When a proton transfers across the hydrogen-bond center, that is, $q_1$ changes from negative to positive values, $q_2$ passes through a minimum when H is located in the center at $q_1 = 0$. In other words, in a first approximation, the hydrogen-bond geometry can be described by a single parameter, such as $q_1$, and $q_2$ can be reconstructed using the general $q_1$ versus $q_2$ correlation. Various spectroscopic observables have been correlated with $q_1$. In ref 35, based on a method described in ref 27, the following equation was proposed to link $q_1$ and bridging-proton chemical shift values

$$\delta H = 6 + 15.3 \exp(6.2 q_1^2) \tag{2}$$

where the chemical shift $\delta$ is in parts per million (ppm) and $q_1$ is in angstroms (Å). Note that, even though $^1$H and $^2$H NMR chemical shifts must be correlated,[36−38] as are the hydrogen-bond geometries of the OHO and ODO isotopologs of a complex,[27] the hydrogen-bond correlations used in this work were not calibrated for deuterium bonds. Moreover, under our experimental conditions, the quality of the $^2$H NMR spectra is significantly lower than that of the $^1$H NMR spectra. Thus, we considered it premature to obtain quantitative data from the reported $^2$H NMR chemical shifts, and herein, we analyze $^1$H chemical shifts only. Taking into account the nature of correlational dependencies, we also note that the changes in interatomic distances from one complex to another within the series are likely to be more precise than the absolute values of these interatomic distances.

Equation 2 can be applied directly to the case of **1** and **3**, generating $q_1$ values, because the degenerate proton tautomerism in **1** and **3** does not affect the $\delta$H values. Values of $q_2$ can be found using the correlation published in ref 27. The resulting distances are collected in Table 4. Hydrogen-bond geometries are temperature-dependent: In **1**, when temperature is decreased from 160 to 120 K, the heavy-atom distance is shortened by 0.004 Å, and the bridging proton moves 0.01 Å toward the H-bond center (in each tautomer). In **3**, upon cooling from 160 to 120 K, the hydrogen bond shortens by 0.002 Å, and $q_1$ decreases by 0.007 Å. A somewhat interesting observation is that the proton positions in the two tautomers of both **1** and **3** are separated by only 0.2 Å, which is comparable to the width of the square of the vibrational wave function of the proton.[39,40] It is plausible that, for such a short proton transfer distance, the concept of proton tautomerism starts

**Table 4. Hydrogen-Bond Geometries $r_{OH}$ and $r_{HO}$ Estimated from $^1$H NMR Chemical Shifts for Complexes 1 and 3 Using H-Bond Correlations[a]**

| complex | $T$ (K) | $r_{OH}$ (Å) | $r_{HO}$ (Å) | $\lvert q_1\rvert = {}^1/_2\lvert r_{OH} - r_{HO}\rvert$ (Å) | $q_2 = r_{OH} + r_{HO}$ (Å) |
|---|---|---|---|---|---|
| **1** | 160 | 1.1043 | 1.3366 | 0.1163 | 2.4409 |
| | 120 | 1.1122 | 1.3242 | 0.1060 | 2.4364 |
| **3** | 160 | 1.1046 | 1.3361 | 0.1158 | 2.4407 |
| | 120 | 1.1084 | 1.3301 | 0.1092 | 2.4385 |

[a] See text for details.

to approach its limits and it is worth considering the whole ensemble of solvatomers without selecting two forms only.

A similar approach to hydrogen-bond geometry estimation can not be used in the cases of **2** and **4** because the bridging-proton chemical shifts of these monoanions are averaged between two unknown intrinsic values with unknown weighting coefficients. Nevertheless, we assume that the main geometric parameters of the hydrogen bonds in **2** and **4** are qualitatively similar to those in **1** and **3**: O···O distances of about 2.4 Å and an average hydrogen-bond asymmetry of about 0.1 Å.

**Integrity of the Hydrogen Bond during Conformational Interconversion.** The conformational interconversion in monoanions **1**, **2**, and **4** could take place through a direct interconversion of the gauche 1 and gauche 2 forms (which might or might not require breaking of the hydrogen bond), or alternatively, the isomerization could pass through the trans form.

First, let us consider the direct interconversion of the gauche forms. To determine whether the H-bond is retained during this process, we performed ab initio calculations (MP2/6-311++G**) of the geometries and energies of the corresponding equilibrium structures and transition states for **1**−**4**. Each calculation was checked by vibrational frequency analysis. The details of these calculations are presented in the Supporting Information (see Figure S1 and Table S1). Here, we report only the final results. We found out that the hydrogen bond is retained during the isomerization and that the energies of the transition states are equal to 9.6, 13.8, and 9.5 kcal/mol for **1**, **2**, and **4**, respectively. This matches well the corresponding activation energies obtained from the line shape analyses of experimental spectra: 8.5, 13.8−14.6, and 8.0 kcal/mol (see Table 3).

The second conformational interconversion pathway involves the formation of the trans isomer and requires breaking of the intramolecular H-bond. By QM calculations, we estimate the energy of hydrogen-bond formation to be 17 kcal·mol$^{-1}$ for **1**, 15 kcal·mol$^{-1}$ for **2**, and 16 kcal·mol$^{-1}$ for **4** (see Supporting Information, Figure S2).

For **1** and **4**, the hydrogen-bond energies are noticeably larger than the experimental conformational interconversion activation energies obtained by the line shape analyses, and we conclude that the trans isomer is not formed during the isomerization. In the case of **1**, the integrity of the H-bond is further supported by the observation of the sharp bridging-proton signal throughout the whole temperature interval from 180 to 120 K.

The possibility of a conformational interconversion through the trans form remains open for **2**. Indeed, the calculated hydrogen-bond strength and the experimental activation energy of the isomerization are similar. This is due to the fact that the direct conversion of the gauche 1 and gauche 2 forms of **2** necessarily passes through the eclipsed conformation of the methyl groups. Note, however, that the calculated hydrogen-bond formation energy for **2** refers to the fully relaxed trans form with only the C−C−C−C dihedral angle fixed, so that any additional energy barriers associated with the eclipsing of carbonyl with methyl groups (in the cases of **2** and **4**) are not taken into account. Further analysis is needed before one of the interconversion pathways can be excluded for **2**.

## SUMMARY

We have studied the monoanions of succinic, methylsuccinic, and *meso*-/*rac*-dimethylsuccinic acids (with tetraalkylammonium as the counterion) dissolved in $CDF_3/CDF_2Cl$ mixture (**1**−**4**, Figure 1). By analysis of the low-temperature $^1H$, $^2H$, and $^{13}C$ NMR spectra, we have shown that all four monoanions form short intramolecular OHO hydrogen bonds (O···O ≈ 2.44 Å, as estimated from the hydrogen-bond correlations[27]). In contrast to well-studied hydrogen maleates and phthalates, the situation in the succinates reflects the conformational flexibility within the carbon skeletons of the molecules: **1**, **2**, and **4** exist as mixtures of two directly interconverting gauche forms. At low temperatures, the interconversion can be slowed on the NMR time-scale. The experimentally observed energy barrier for this process is 10−15 kcal/mol, which is in good agreement with calculated values (MP2/6-311++G**). In **3**, the conformational interconversion is hindered by the steric repulsion of the methyl groups.

The symmetry and geometry of the intramolecular hydrogen bond depend on the substituents. In **1** and **3**, the proton is located in a symmetric double-well potential, jumping rapidly by ca. 0.22 Å between two degenerate positions. In **2**, the asymmetry of the H-bond is created by the dihedral C−C−C−C angle; the bridging proton predominantly resides close to one of the carboxylic groups, and the conformational interconversion is associated with a transfer of this proton. Monoanion **4** bears the lowest symmetry among the studied complexes. In one of its gauche conformers (marked with a single asterisk in Figure 5), H/D isotope effects on the chemical shift of the carboxylic carbon indicate significant proton tautomerism, whereas in the other gauche form (marked with two asterisks), the bridging proton is located predominantly close to one of the carboxylic groups, similarly to what was found for **2**.

It is surprising how strongly the $^{13}C$ NMR chemical shift of carboxylic group depends on the C−C−C−C dihedral angle. In a formally symmetric monoanion **2**, the two carboxylates are chemically inequivalent primarily because of the nonplanarity of the molecular skeleton, and their chemical shifts differ by 4 ppm, which is almost the entire span of chemical shifts between neutral and deprotonated carboxylic groups. This finding might be of significance for the studies of proteins, where the changes in the $^{13}C$ NMR chemical shifts of glutamic and aspartic acid side chains are often interpreted as protonation/deprotonation of the carboxylic group.

## ASSOCIATED CONTENT

**Supporting Information.** Calculated relative stabilities and optimized structures of conformational isomers and proton tautomers, as well as transition states between them, for species **1**−**4**; list of *r*(O···H), *r*(H···O), and *r*(O···O) distances and OHO angles. Hydrogen-bond energies for **1**−**4**, estimated as the energy differences between the fully optimized structures and the corresponding trans isomers. This information is available free of charge via the Internet at http://pubs.acs.org.

## AUTHOR INFORMATION

**Corresponding Author**
*E-mail: tolstoy@chemie.fu-berlin.de.

## ACKNOWLEDGMENT

This work was supported by the Deutsche Forschungsgemeinschaft, Bonn, Germany; the Fonds der Chemischen Industrie, Frankfurt, Germany; and the Russian Foundation of Basic Research.

## REFERENCES


(1) Perrin, C. L.; Nielson, J. B. *J. Am. Chem. Soc.* **1997**, *119*, 12734–12741.
(2) Perrin, C. L. *Acc. Chem. Res.* **2010**, *43*, 1550–1557.
(3) Drobez, S.; Golic, L.; Leban, I. *Acta Crystallogr.* **1985**, *C41*, 1503–1505.
(4) Madsen, D.; Flensburg, C.; Larsen, S. *J. Phys. Chem. A* **1998**, *102*, 2177–2188.
(5) Harte, S. M.; Parkin, A.; Goeta, A.; Wilson, C. C. *J. Mol. Struct.* **2005**, *741*, 93–96.
(6) Langkilde, A.; Madsen, D.; Larsen, S. *Acta Crystallogr.* **2004**, *B60*, 502–511.
(7) Fillaux, F.; Leygue, N.; Tomkinson, J.; Cousson, A.; Paulus, W. *Chem. Phys.* **1999**, *244*, 387–403.
(8) Perrin, C. L. *Science* **1994**, *266*, 1665–1668.
(9) Perrin, C. L.; Lau, J. S. *J. Am. Chem. Soc.* **2006**, *128*, 11820–11824.
(10) Kidric, J.; Mavri, J.; Podobnik, M.; Hadzi, D. *J. Mol. Struct.* **1990**, *237*, 265–271.
(11) Schah-Mohammedi, P.; Shenderovich, I. G.; Detering, C.; Limbach, H.-H; Tolstoy, P. M.; Smirnov, S. N.; Denisov, G. S.; Golubev, N. S. *J. Am. Chem. Soc.* **2000**, *122*, 12878–12879.
(12) (a) Steiner, Th.; Saenger, W. *Acta Crystallogr.* **1994**, *B50*, 348–357. (b) Steiner, Th. *J. Chem. Soc., Chem. Commun.* **1995**, 1331–1332. (c) Gilli, P.; Bertolasi, V.; Ferretti, V.; Gilli, G. *J. Am. Chem. Soc.* **1994**, *116*, 909–915. (d) Steiner, Th. *J. Phys. Chem. A* **1998**, *102*, 7041–7052.
(13) Kashino, S.; Taka, J.; Yoshida, T.; Kubozono, Y.; Ishida, H.; Maeda, H. *Acta Crystallogr.* **1998**, *B54*, 889–894.
(14) Kalsbeek, N. *Acta Crystallogr.* **1991**, *C47*, 1649–1653.
(15) Schouwstra, Y. *Acta Crystallogr.* **1972**, *B28*, 2217–2221.
(16) Price, D. J.; Roberts, J. D.; Jorgensen, W. L. *J. Am. Chem. Soc.* **1998**, *120*, 9672–9679.
(17) Rudner, M. S.; Jeremic, S.; Petterson, K. A.; Kent, D. R.; Brown, K. A.; Drake, M. D.; Goddard, W. A.; Roberts, J. D. *J. Phys. Chem. A* **2005**, *109*, 9076–9082.
(18) Smith, A. A.; Drake, M. D.; Rahim, A. K.; Roberts, J. D. *J. Phys. Chem. A* **2008**, *112*, 12367–12371.
(19) Retey, J.; Hull, W. E.; Snatzke, F.; Snatzke, G.; Wagner, U. *Tetrahedron* **1979**, *35*, 1845–1849.
(20) Cassidy, C. S.; Lin, J.; Tobin, J. B.; Frey, P. A. *Bioorg. Chem.* **1998**, *26*, 213–219.
(21) Perrin, C. L.; Thoburn, J. D. *J. Am. Chem. Soc.* **1992**, *114*, 8559–8565.
(22) Roberts, J. D. *Acc. Chem. Res.* **2006**, *39*, 889–896.
(23) Smith, R.; Brereton, I. M.; Chai, R. Y.; Kent, S. B. H. *Nat. Struct. Biol.* **1996**, *3*, 946–950.
(24) Perrin, C. L.; Lau, J. S.; Kim, Y.-J.; Karri, P.; Moore, C.; Rheingold, A. L. *J. Am. Chem. Soc.* **2009**, *131*, 13548.
(25) Tolstoy, P. M.; Schah-Mohammedi, P.; Smirnov, S. N.; Golubev, N. S.; Denisov, G. S.; Limbach, H.-H. *J. Am. Chem. Soc.* **2004**, *126*, 5621–5634.
(26) Tolstoy, P. M.; Guo, J.; Koeppe, B.; Golubev, N. S.; Denisov, G. S.; Smirnov, S. N.; Limbach, H.-H. *J. Phys. Chem. A* **2010**, *114*, 10775–10782.
(27) Limbach, H.-H.; Tolstoy, P. M.; Pérez-Hernández, N.; Guo, J.; Shenderovich, I. G.; Denisov, G. S. *Israel J. Chem.* **2009**, *49*, 199–216.
(28) Siegel, J. S.; Anet, F. A. L. *J. Org. Chem.* **1988**, *53*, 2629–2630.
(29) Frisch, M. J.; Trucks, G. W.; Schlegel, H. B.; Scuseria, G. E.; Robb, M. A.; Cheeseman, J. R.; Montgomery, J. A., Jr.; Vreven, T.; Kudin, K. N.; Burant, J. C.; Millam, J. M.; Iyengar, S. S.; Tomasi, J.; Barone, V.; Mennucci, B.; Cossi, M.; Scalmani, G.; Rega, N.; Petersson, G. A.; Nakatsuji, H.; Hada, M.; Ehara, M.; Toyota, K.; Fukuda, R.; Hasegawa, J.; Ishida, M.; Nakajima, T.; Honda, Y.; Kitao, O.; Nakai, H.; Klene, M.; Li, X.; Knox, J. E.; Hratchian, H. P.; Cross, J. B.; Bakken, V.; Adamo, C.; Jaramillo, J.; Gomperts, R.; Stratmann, R. E.; Yazyev, O.; Austin, A. J.; Cammi, R.; Pomelli, C.; Ochterski, J. W.; Ayala, P. Y.; Morokuma, K.; Voth, G. A.; Salvador, P.; Dannenberg, J. J.; Zakrzewski, V. G.; Dapprich, S.; Daniels, A. D.; Strain, M. C.; Farkas, O.; Malick, D. K.; Rabuck, A. D.; Raghavachari, K.; Foresman, J. B.; Ortiz, J. V.; Cui, Q.; Baboul, A. G.; Clifford, S.; Cioslowski, J.; Stefanov, B. B.; Liu, G.; Liashenko, A.; Piskorz, P.; Komaromi, I.; Martin, R. L.; Fox, D. J.; Keith, T.; Al-Laham, M. A.; Peng, C. Y.; Nanayakkara, A.; Challacombe, M.; Gill, P. M. W.; Johnson, B.; Chen, W.; Wong, M. W.; Gonzalez, C.; Pople, J. A. *Gaussian 03*, revision B.04: Gaussian, Inc.: Pittsburgh, PA, 2003.
(30) The MEXICO Suite of Programs for NMR Chemical Exchange Lineshape Calculation, version 3.0. Available at http://www.chemistry.mcmaster.ca/bain/exchange.html. Accessed July 2011.
(31) gNMR License Agreement. Available at http://home.cc.umanitoba.ca/~budzelaa/gNMR/gNMR-license.html.
(32) Detering, C.; Tolstoy, P. M.; Golubev, N. S.; Denisov, G. S.; Limbach, H.-H. *Dokl. Phys. Chem.* **2001**, *379*, 1–4.
(33) Golubev, N. S.; Melikova, S. M.; Shchepkin, D. N.; Shenderovich, I. G.; Tolstoy, P. M.; Denisov, G. S. *Z. Phys. Chem.* **2003**, *217*, 1549–1563.
(34) Facelli, J. C.; Gu, Z.; McDermott, A. *Mol. Phys.* **1995**, *86*, 865–872.
(35) Guo, J.; Koeppe, B.; Tolstoy, P. M. *Phys. Chem. Chem. Phys.* **2011**, *13*, 2335.
(36) Chmielewski, P.; Ozeryanskii, V. A.; Sobczyk, L.; Pozharskii, A. F. *J. Phys. Org. Chem.* **2007**, *20*, 643–648.
(37) Golubev, N. S.; Detering, C.; Smirnov, S. N.; Shenderovich, I. G.; Denisov, G. S.; Limbach, H.-H.; Tolstoy, P. M. *Phys. Chem. Chem. Phys.* **2009**, *11*, 5154–5159.
(38) Ando, K. *Phys. Rev. B* **2005**, *72*, 172104.
(39) Garcia-Viloca, M.; Gonzalez-Lafont, A.; Lluch, J. M. *J. Am. Chem. Soc.* **1999**, *121*, 9198–9207.
(40) Steiner, T.; Majerz, I.; Wilson, C. C. *Angew. Chem., Int. Ed.* **2001**, *40*, 2651–2654.